All-optical cooling of Fermi gases via Pauli inhibition of spontaneous emission

Roberto Onofrio

Dipartimento di Fisica e Astronomia "Galileo Galilei," Università di Padova, Via Marzolo 8, Padova 35131, Italy
and Department of Physics and Astronomy, Dartmouth College, 6127 Wilder Laboratory, Hanover, New Hampshire 03755, USA

(Received 27 October 2015; published 21 March 2016)

A technique is proposed to cool Fermi gases to the regime of quantum degeneracy based on the expected inhibition of spontaneous emission due to the Pauli principle. The reduction of the linewidth for spontaneous emission originates a corresponding reduction of the Doppler temperature, which under specific conditions may give rise to a runaway process through which fermions are progressively cooled. The approach requires a combination of a magneto-optical trap as a cooling system and an optical dipole trap to enhance quantum degeneracy. This results in expected Fermi degeneracy factors T/T_F comparable to the lowest values recently achieved, with potential for a direct implementation in optical lattices. The experimental demonstration of this technique should also indirectly provide a macroscopic manifestation of the Pauli exclusion principle at the atomic physics level.

DOI: 10.1103/PhysRevA.93.033414

I. INTRODUCTION

One of the current goals of ultracold atom physics is to reach deeper quantum degeneracy for Fermi gases, which could enable the study of new phases of matter otherwise prevented by thermal effects [1–3]. The adaptation of evaporative cooling techniques so successful in the case of Bose gases to Fermi gases has been proven to be challenging, and so far the best degeneracy factors achieved have been in the $T/T_F \simeq 0.03$–0.05 range [4,5]. Physically, the origin of this plateau is rooted in the intrinsic difference between bosons and fermions. For the former, a cooling technique based on many-body effects such as evaporative cooling seems favorable as bosons tend to bunch in the same region of phase space and energy. Fermions instead manifest the opposite behavior, hence the lack of spatial overlap creates increasing difficulty as the degenerate regime is approached, further creating peculiar sources of heating [6]. Limits to the efficiency of dual evaporative cooling between two distinguishable components of a Fermi gas have been discussed [7,8] and found to be in line with previous experimental findings [9]. A compromise may consist in using sympathetic cooling of Fermi gas via Bose gases but, as noticed in [10], the diminished heat capacity of a Bose gas at the onset of Bose-Einstein condensation makes sympathetic cooling increasingly inefficient. Although techniques to mitigate this limitation using species-selective traps have been proposed [11,12] and implemented in the Bose counterparts [13,14], their broad application to reach quantum degeneracy in Fermi-Bose mixtures remains pending, with the notable exception of a very recent report on Yb-Rb mixtures [15].

Considering that a decade-long effort has not yet resulted in appreciable progress in Fermi cooling, one may ask whether it is possible to envision other cooling techniques which may transform the shortcomings of a Fermi gas into assets. In this paper, we discuss such a possibility by exploiting a well-known *individual* cooling technique, Doppler cooling in a magneto-optical trap (MOT), and a *collective* effect unique of Fermi systems, the narrowing of the spontaneous emission linewidth. The analysis is first carried out on an atomic gas confined in a magneto-optical trap to illustrate the basics of the effect, as discussed in Sec. II. The limitations of Doppler cooling for fermionic isotopes of alkali-metal atoms bring a more elaborated setup consisting in a hybrid configuration in which cooling is still ensured by the MOT, and trapping is achieved by a stiff optical dipole trap (ODT), as discussed in Sec. III. In Sec. IV we focus on the limitations to the cooling capability due to heating sources, and we discuss estimates of heating due to Rayleigh scattering in the ODT, showing that this should not compromise the achievement of quantum degeneracies comparable to the ones currently achieved with other cooling techniques. Advantages and drawbacks of the proposal are then discussed in the conclusions, with particular regard to its implementation in optical lattices.

II. COOLING BY PROGRESSIVE SUPPRESSION OF THE SPONTANEOUS-EMISSION LINEWIDTH

It is well known that in the strongly degenerate regime a Fermi gas is expected to manifest inhibition of spontaneous emission [16–21]. As discussed in [19], three energy scales compete in determining the inhibition: the Fermi energy E_F, the recoil energy $E_R = 2\pi\hbar^2/(2m\lambda_{\rm at}^2)$ (with $\lambda_{\rm at}$ the wavelength of the Doppler cooling cycling transition), and the average thermal energy $k_B T$, with k_B denoting the Boltzmann constant. Under the restrictions dictated by the Pauli principle, single-particle states in the energy range $E_F - k_B T \leqslant E \leqslant E_F + k_B T$ are partially occupied, so they can still accept an atom which undergoes spontaneous emission provided that its motional energy (given on average by the recoil energy plus the always present bonus of thermal energy, i.e., $E_R + k_B T$) falls in the same energy range. If, however, the Fermi energy is made too large with respect to E_R and $k_B T$, the transition becomes progressively unlikely, as the motional energy is not enough to allow hopping into the energy levels still partially occupied. This effect has been studied quantitatively via explicit evaluation of the matrix element with numerical techniques [19], and with a local density approximation [21]. With reference to this last approximation, if Γ_0 and Γ denote the intrinsic spontaneous emission linewidth and the spontaneous emission linewidth including the effect of the Pauli principle, respectively, then the spontaneous emission

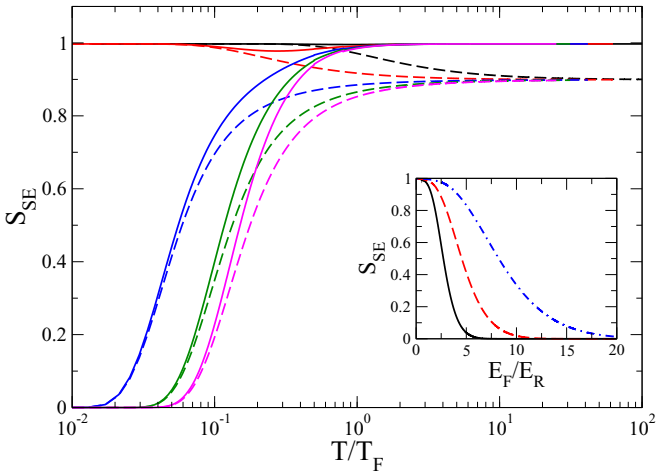

FIG. 1. Inhibition of the spontaneous emission for a Fermi gas. The spontaneous emission suppression factor $S_{\rm SE}$ is plotted versus the degeneracy factor T/T_F for different values of the Fermi energy in units of the recoil energy, from top to bottom curves, $E_F/E_R = 0.4$ (black), $E_F/E_R = 0.8$ (red), $E_F/E_R = 1.2$ (blue), $E_F/E_R = 1.6$ (green), and $E_F/E_R = 2.0$ (magenta). The continuous lines are evaluated assuming a temperature-dependent chemical potential, while the dashed lines are obtained by using the approximation $\mu = E_F$ valid only at low T/T_F (see also Fig. 1 of [21]). In the inset the complementary dependence of $S_{\rm SE}$ upon the E_F/E_R ratio at constant temperature is shown for values $k_BT/E_R = 0.5$ (black, continuous), $k_BT/E_R = 1$ (red, dashed), and $k_BT/E_R = 2$ (blue, dot-dashed).

suppression factor $S_{\rm SE} = \Gamma/\Gamma_0$ is [21]

$$S_{\rm SE} \simeq z^{-1}\exp(\xi^2) f_3(ze^{-\xi^2}), \tag{1}$$

where $z = \exp(\beta\mu)$ is the fugacity of the Fermi gas, with $\beta = (k_BT)^{-1}$ its inverse temperature, μ the chemical potential, $\xi = \sqrt{\beta E_R}$, and f_3 belongs to the set of functions defined in general in terms of the Fermi integral

$$f_\nu(y) = \frac{1}{\Gamma(\nu)}\int_0^\infty dx \frac{x^{\nu-1}}{\exp(x/y)+1}, \tag{2}$$

evaluated in the specific case of $\nu = 3$, where $\Gamma(\nu)$ is the gamma function.

The dependence of $S_{\rm SE}$ on the degeneracy factor T/T_F is shown through the continuous lines in Fig. 1, for various values of the ratio E_F/E_R. The chemical potential of the Fermi gas has been evaluated at all temperatures with a function interpolating between the two extreme limits of the Sommerfeld expansion,

$$\mu = E_F\left\{1 - \left[\pi k_BT/(\sqrt{3}E_F)\right]^2\right\}, \tag{3}$$

and the high-temperature limit

$$\mu = -k_BT\ \ln[6(k_BT/E_F)^3]. \tag{4}$$

The dashed lines in Fig. 1 are instead evaluated through the Sommerfeld approximation with the chemical potential equal to the Fermi energy, $\mu = E_F$, only valid at low T/T_F. The expected failure of this approximation at high temperature is manifested through an asymptotic value of $S_{\rm SE} \simeq 0.9$ for $T \to \infty$ and more optimistic values of the suppression factor at any finite temperature. The curves show that inhibition of spontaneous emission is ineffective at low values of E_F/E_R, and that it becomes progressively less sensitive to E_F/E_R when this ratio becomes much larger than unity, an effect corroborated by showing its explicit dependence as in the inset of Fig. 1.

The analysis of the plots suggests that, if the initial temperature is such that there is already some degree, even if small, of quantum degeneracy, i.e., $T \lesssim T_F$, the linewidth Γ should become slightly smaller than its intrinsic value Γ_0, and consequently the Doppler limit temperature $T_D = \hbar\Gamma/2k_B$ would be shifted to a smaller value, which also implies that the lowest temperature achieved during Doppler cooling will become smaller. This in turn implies a smaller degeneracy factor T/T_F, which implies a smaller Γ and then again a smaller Doppler limit temperature. This loop will continue until the Doppler temperature becomes of the same order of magnitude of the recoil temperature.

This iterative dynamics can be made explicit with a simple recursive relationship in which each time step is of the order of the spontaneous emission lifetime $\tau = 1/\Gamma = 1/(S_{\rm SE}\Gamma_0)$, and we assume that equilibration time scales are comparable to this parameter. The temperature of the atomic cloud after the Nth time step is then

$$T_{N+1} = S_{\rm SE}(T_N/T_F)T_N, \tag{5}$$

where we indicate the explicit dependence on T_F even if for now we consider a situation in which E_F is kept constant. It is clear from this simple relationship and the plots in Fig. 1 that there is a fixed point corresponding to zero temperature. In Fig. 2(a) we show the dynamics due to the iterative mapping of Eq. (3) for a Fermi gas precooled to the recoil limit temperature, that is, with initial temperature equal to E_R/k_B. Due to the highly nonlinear behavior of the iterative map, the temperature becomes extremely sensitive to the initial value of E_F/E_R and the number of iterations. The fastest cooling trajectory shown in Fig. 2(a) occurs for $E_F/E_R = 2$, in which a dozen iterations appear to be enough to reach $T/T_F \leqslant 10^{-2}$. Conversely, about 10^3 iterations are required to reach $T/T_F \simeq 0.1$ if $E_F/E_R = 0.4$, which is also aggravated by the fact that the actual time step is not uniform, but depends itself upon the degree of Fermi degeneracy. Indeed, being the spontaneous lifetime inversely proportional to the transition linewidth, the actual times for cooling and equilibration of a more degenerate cloud becomes proportionately longer, and the equally spaced steps in the horizontal axis of Fig. 2(a) should be replaced by time intervals of amplitude $\tau_N = 1/[S_{\rm SE}(T_N/T_F)\Gamma_0]$. In Fig. 2(b) we show the complementary dependence of T/T_F upon the number of iterations keeping constant the E_F/E_R ratio and varying the initial temperature, giving information on the sensitivity of the iterative scheme upon initial states with temperature higher than the recoil temperature. Alternatively, the iterative relationship in Eq. (5) can be easily converted into a differential equation keeping in mind that the time scale for cooling is of the order of the spontaneous emission lifetime,

$$\frac{dT}{dt} \simeq \frac{T_{N+1}-T_N}{\tau_N} = -S_{\rm SE}(1-S_{\rm SE})\Gamma_0 T, \tag{6}$$

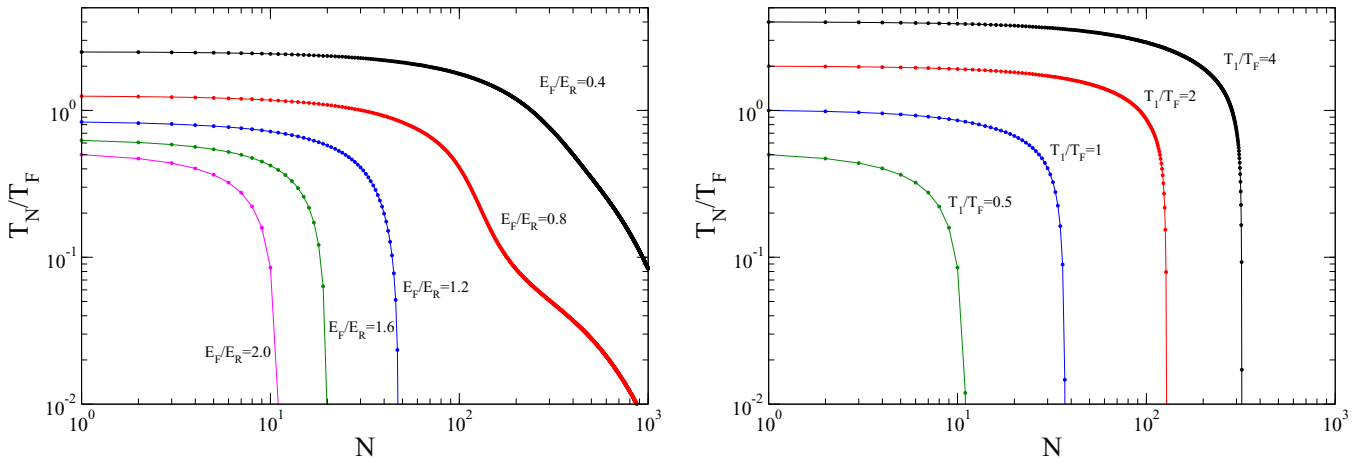

FIG. 2. Pauli cooling dynamics as based on the iterative equation (5). (a) Degeneracy factor T_N/T_F versus the number of iterations for the same values of the E_F/E_R ratio used in Fig. 1. The initial temperature is assumed to be equal to the recoil temperature, as expected at the end of a MOT cooling protocol also exploiting a stage with optical molasses. (b) Degeneracy factor T_N/T_F versus number of iterations for $E_F/E_R = 2$ and different initial temperatures T_1, with the curve at the bottom (for $T_1/T_F = 0.5$) corresponding to an initial temperature equal to the recoil temperature, $T_1 = E_R/k_B$.

in which an effective cooling time scale may be identified as $\tau_{\rm cool} = [S_{\rm SE}(1 - S_{\rm SE})\Gamma_0]^{-1}$ depending on the degeneracy parameter T/T_F and then on time, confirming that the dynamics is highly nonlinear. The maximal cooling speed is achieved in the intermediate regime $S_{\rm SE} \simeq 1/2$, while it tends to zero both in the case of $S_{\rm SE}$ close to unity—i.e., far from quantum degeneracy, when the linewidth suppression is not present—and when $S_{\rm SE}$ is close to zero, i.e., when the spontaneous lifetime tends to infinity slowing down the cooling process. In Fig. 3 we show the implications in terms of the time dependence of the degeneracy parameter for the same iterative scheme discussed in Fig. 2(a), and the spontaneous emission lifetime of the dominant transition $2s_{1/2}$-$2p_{3/2}$ in

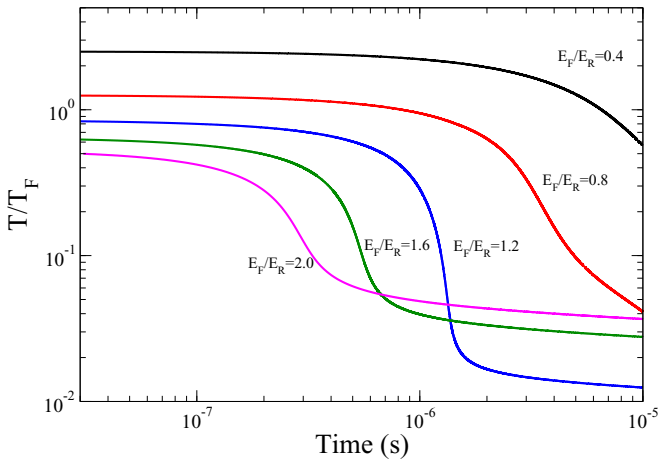

FIG. 3. Same case as in Fig. 2(a) but with the actual time in abscissa, with the time evolution ruled by Eq. (6). Although it seems that even for moderate values of the E_F/E_R ratio the degeneracy factor decreases, this occurs at the price of a much slower time scale with respect to the case of large E_F/E_R ratios. Notice that too large E_F/E_R ratios imply large spontaneous lifetimes achieved at early times, which results in precocious slowdown of the cooling dynamics, as visible especially for the $E_F/E_R = 2$ case.

^{6}Li ($\lambda_{\rm at} = 671$ nm, $\Gamma = 2\pi \times 5.9$ MHz). While all curves show $T/T_F \to 0$ as $t \to \infty$, their behavior at finite time is different, with the appearance of an optimal, intermediate value of E_F/E_R leading to maximum cooling, a situation of interest in any realistic scheme, in which obviously a nonzero cooling power is required.

III. COOLING IN A MOT ASSISTED BY AN OPTICAL DIPOLE TRAP

The previous analysis has shown that the initial degeneracy parameter T/T_F is crucial to ignite the expected runaway process, as specifically seen in Fig. 2(b). In applications to specific Fermi gases, with ^{6}Li and ^{40}K being the only alkali-metal stable or long lifetime fermionic isotopes, the temperature is initially limited by the Doppler temperature itself due to the unresolved hyperfine structure preventing efficient optical molasses cooling. This issue is generally not present in alkaline-earth-metal fermionic species, for which the starting point can be a sub-Doppler temperature, which in the presence of a degeneracy parameter T/T_F small enough can start the runaway process until the Doppler temperature reaches the recoil temperature. We deliberately address in the following the less favorable situation of ^{6}Li and ^{40}K, also due to their widespread availability in several laboratories. The cooling process can be made more efficient in spite of the absence of genuine sub-Doppler cooling stages by both increasing its speed, related to the E_F/E_R ratio as visible in Fig. 2(a), and decreasing the T/T_F ratio. This is simultaneously achieved by adding an ODT sharing the same potential energy minimum as the MOT, which will increase the Fermi energy thereby decreasing T/T_F while increasing E_F/E_R. In this condition, the achievement of a temperature close to the recoil temperature is no longer a strong limitation, as far as we are concerned with getting the minimum T/T_F and not minimum temperatures in an absolute sense. Fortunately, most of the interesting phase transition physics depends on the entropy, which in turn depends on the T/T_F ratio.

The coexistence of a MOT only utilized for Doppler cooling and an ODT for stiff trapping is not an issue provided that the laser wavelength for the ODT is judiciously chosen to avoid any ac Stark shift of the two levels realizing the cycling cooling transition in the MOT, as achievable by using the so-called magic wavelengths [22,23]. Production of large degenerate samples of ^{6}Li has been recently reported in [24], to which we also refer for discussions of experimental details, in which the authors have reported efficient Doppler and molasses cooling in the presence of the strong light field of the ODT.

We focus here on the case of ^{6}Li, and a crossed ODT produced by a laser working at one magic wavelength for the relevant ^{6}Li cyclic transition. The trapping frequencies along the three axes may be written as

$$\omega_x = \omega_y = \frac{\omega_z}{\sqrt{2}} = \left(\frac{\hbar\alpha P}{\pi m w^4}\right)^{1/2}, \tag{7}$$

where P is the instantaneous laser power, w the waist of the laser beam, $\alpha = \Gamma^2/\{[1/(\Omega_{\rm at} - \Omega_{\rm las})]I_{\rm sat}\}$, where $I_{\rm sat} = \hbar\Omega_{\rm at}^3\Gamma/(12\pi c^2)$ is the saturation intensity, with $\Omega_{\rm at} = 2\pi c/\lambda_{\rm at}$, $\Omega_{\rm las} = 2\pi c/\lambda_{\rm las}$, and $\lambda_{\rm at}$ and $\lambda_{\rm las}$ the atomic transition and laser wavelength, respectively. The case of the crossed ODT, although more difficult to achieve due to the need of focusing two laser beams on the MOT center, is the closest to isotropy and avoids excessive spatial mismatching with respect to the preexisting shape of the atomic cloud in the MOT. Also, in order to avoid sudden heating of the atomic cloud, the initial laser power should be chosen appropriately to allow for a smooth transition from the MOT trapping to the ODT trapping, thereby the need to start with a moderate value of the laser power then progressively ramped up. The linear dependence of the Fermi energy on the average trapping frequency $\omega = (\omega_x\omega_y\omega_z)^{1/3}$, as $E_F = 1.82\hbar\omega N_F^{1/3}$, and the fact that the average trapping frequency scales as $P^{1/2}$ implies a scaling of the degeneracy parameter as $T/T_F \propto P^{-1/2}$.

The effect of the ODT on the iterative scheme is shown in Fig. 4 for various laser powers and two different cyclic transitions. The case of the $2s_{1/2}$-$3p_{3/2}$ cyclic transition seems apparently more suitable, since in this case the spontaneous emission linewidth is narrower, and in fact slightly larger than the recoil temperature, making the initial conditions more appealing for Pauli cooling. However, due to the dependence of the trapping frequencies on the linewidth and the saturation intensity, the initial confinement is weaker than in the alternative situation of the $2s_{1/2}$-$2p_{3/2}$ cyclic transition, if the comparison is made for the same laser power and waist. This weaker trapping slows down the cooling process so much that, as seen in Fig. 4, the gain in T/T_F is only due to the ramping of the laser power and the increase in T_F, rather than the intrinsic decrease of T. Conversely, in the case of the $2s_{1/2}$-$2p_{3/2}$ transition, the cooling is more effective and reaches the recoil limit well before the laser power is settled at a constant value after 10^2 iterations, at which point further gains in the T/T_F ratio are only achieved by increasing T_F. The case of a constant and shallow ($P = 10$ W) optical trap is also shown, to emphasize both the gain in speed and in the achievable mimimum T/T_F ratio by using time-dependent laser powers.

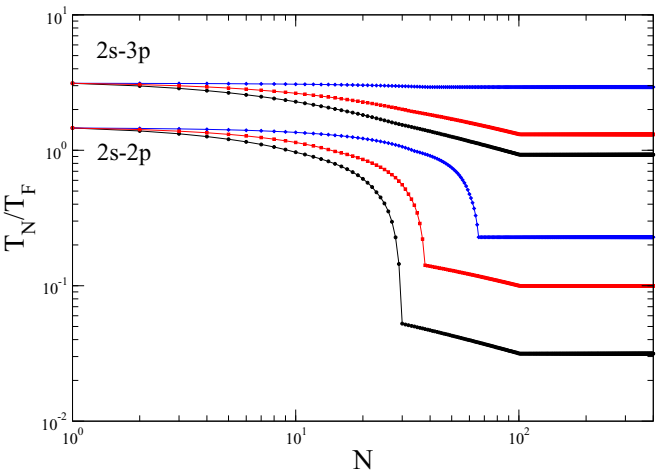

FIG. 4. Pauli cooling of a Fermi gas in a hybrid combination of a magneto-optical trap and an optical dipole trap. The three bottom curves show the effect of the optical dipole trap for trapping and cooling 10^5 ^{6}Li atoms in the three cases of constant laser power (blue diamonds, dot-dashed) of $P = 10$ W, and a linear ramp starting from the initial time until 10^2 iterations with the same initial value of 10 W and final value of 50 W (red squares, dashed) and 100 W (black circles, continuous), with a beam waist $w = 20$ μm. The initial temperature of the atoms is assumed to be the Doppler temperature for the $2s_{1/2}$-$2p_{3/2}$ cyclic transition, $T_D = 140$ μK, and the laser wavelength is assumed to be $\lambda_{\rm las} = 930.3$ nm, minimizing the Stark shifts induced by the ODT. The three top curves are relative to the case of a $2s_{1/2}$-$3p_{3/2}$ cyclic transition with the initial temperature assumed to be the corresponding Doppler temperature of $T_D = 18$ μK, a laser wavelength of $\lambda_{\rm las} = 1070.73$ nm, and the same laser power trajectories as for the $2s_{1/2}$-$2p_{3/2}$ cyclic transition. Due to the weaker optical confinement as a consequence of the smaller linewidth Γ, the latter cyclic transition is not favorable despite a smaller initial Doppler temperature.

IV. LIMITATIONS TO COOLING DUE TO HEATING SOURCES

An obvious limitation in the use of a high power ODT is due to the concurring heating rate by off-resonant Rayleigh scattering. Also, higher densities of the Fermi gas will make molecule formation more likely, and with it a faster decay of the atomic gas through three-body collisions and related processes. In Fig. 5 we show the impact on the cooling scheme of two additional limiting factors. First, the ODT introduces a heating source due to Rayleigh scattering. Although the off-resonance nature of the laser beam should limit this heating source, the effect may significantly affect the cooling efficiency in the latest stages due to the linear dependence of the specific heat of a Fermi gas on the T/T_F ratio, which makes the atomic gas more susceptible to any heating source. Second, as anticipated in Sec. II, in a realistic modeling the iteration steps should be replaced by the actual time interval occurring for each step, which depends on the spontaneous lifetime and the suppression factor $S_{\rm SE}$. This is a further limitation to the cooling scheme since it slows down the dynamics, while Rayleigh scattering heating (although suppressed by quantum degeneracy) and any other source of heating are present. The specific heat per unit of atom has been evaluated interpolating between

the degenerate regime and the Dulong-Petit limit with an exponential function $C_F = 3k_B\{1 - \exp[-\pi^2 k_B T/(3E_F)]\}$. The dramatic time dependence of the case with final power of 100 W shows that, once a deep Fermi degeneracy is reached, the time scale slows down significantly. This implies a large exposure to Rayleigh heating, further enhanced by the decreased specific heat—thereby the sudden jump, in the next iteration, to much higher degeneracy factors.

The plots show that there is a minimum in the degeneracy factor T/T_F achieved when the cooling and heating rates compensate each other. To avoid the detrimental stage occurring after this minimum, the laser power should be accordingly decreased, thereby allowing for an additional stage of evaporative cooling.

The presence of a minimum achievable value for T/T_F can also be evidenced by analytical estimates completing the differential equation (6) to include the heating source,

$$\frac{dT}{dt} = \dot{T}_{\rm cool} + \dot{T}_{\rm heat} = -S_{\rm SE}(1 - S_{\rm SE})\Gamma_0 T + \frac{P_{\rm heat}}{C_F}, \qquad (8)$$

where $P_{\rm heat}$ is the heating power, and it should be remarked that both $S_{\rm SE}$ and C_F depend upon the degeneracy factor T/T_F, yielding a highly nonlinear dynamics. The heating term is independent of temperature in the Dulong-Petit nondegenerate regime, $\dot{T}_{\rm heat} \simeq P_{\rm heat}/3k_B$, while it increases in inverse proportion to the degeneracy factor in the fully degenerate regime, $\dot{T}_{\rm heat} \simeq P_{\rm heat}/(\pi^2 k_B)E_F/(k_B T)$. Therefore the most delicate stage for heating occurs at later times, when the linearly decreasing specific heat makes the atomic temperature increasingly susceptible to the presence of heating sources. Likewise, as noted earlier the optimal cooling situation is achieved if the spontaneous scattering suppression factor is $S_{\rm SE} = 1/2$, i.e., when the system is in an intermediate quantum degeneracy regime, and in this situation $\dot{T}_{\rm cool} = -\Gamma_0 T/4$. Under this intermediate regime, the balance between cooling and heating rates becomes rather simple, leading to a rough estimate of the minimum degeneracy factor achievable if the limitation is due to heating sources as

$$\left(\frac{T}{T_F}\right)_{\rm min} \simeq 2\pi\left(\frac{P_{\rm heat}}{\Gamma_0 E_F}\right)^{1/2}. \qquad (9)$$

We consider the case of heating power due to residual Rayleigh scattering in the ODT alone, so $P_{\rm heat} = 2\gamma_{\rm sc}\tilde{E}_R$, where

$$\gamma_{\rm sc} = \frac{\Gamma^3}{8}\left(\frac{1}{\Omega_{\rm at} - \Omega_{\rm las}} + \frac{1}{\Omega_{\rm at} + \Omega_{\rm las}}\right)^2\left(\frac{\Omega_{\rm las}}{\Omega_{\rm at}}\right)^3\frac{I}{I_{\rm sat}} \qquad (10)$$

is the scattering rate and $\tilde{E}_R = 2\pi\hbar^2/(2m\lambda_{\rm las}^2)$ is the recoil energy due to the scattering of photons from the ODT laser beams. Notice that, due to the linear dependence on Γ of $I_{\rm sat}$, the heating power depends quadratically on Γ and then on the spontaneous suppression factor $S_{\rm SE}$, making its contribution smaller in the degenerate regime, partially compensating for the larger temperature changes due to the linear drop of the specific heat of the Fermi gas.

For the case of ^{6}Li $2s_{1/2}$-$2p_{3/2}$ transition and power and waist of the ODT laser beams, respectively, of 10 W and 20 μm as in the example in Fig. 4, this gives rise to a lower bound of $k_B T/E_F \simeq 4 \times 10^{-5}$. This is not the actual limiting factor

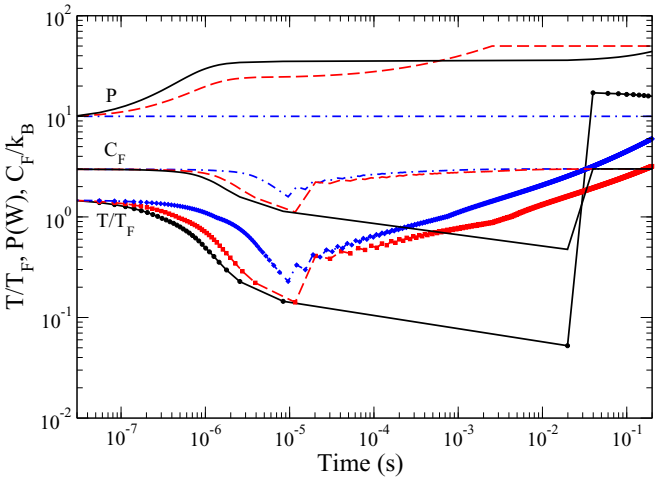

FIG. 5. Time dependence of the degeneracy factor T/T_F in the presence of heating due to Rayleigh scattering from the optical dipole trap. The parameters and the protocols are the same as for the $2s_{1/2}$-$2p_{3/2}$ cyclic transition discussed in Fig. 3. Plotted are the time dependence of the laser power (top curves) for a constant power of 10 W (blue, dot-dashed), a linear ramp from 10 to 50 W then kept constant (red, dashed), and a linear ramp from 10 to 100 W then kept constant (black, continuous), the related specific heats in Boltzmann constant units (middle curves), and the resulting T/T_F trajectories (bottom curves).

since the recoil limit $k_B T_R/E_F \simeq 4 \times 10^{-2}$, in line with what is observed in Fig. 5, is larger by three orders of magnitude. Moreover, the bound expressed by Eq. (9) yields values of T/T_F for which the initial hypothesis of $S_{\rm SE} = 1/2$ does not hold, as a visual inspection of Fig. 1 shows that for the estimated T/T_F we get $S_{\rm SE} \ll 1/2$. Therefore, the analytical estimate in Eq. (9) should be considered as a lower bound on the minimum achievable T/T_F due to heating sources, and its value is also in comparing how the two limitations in T/T_F depend upon the laser power, the waist of the beams, and the number of fermions, as shown in Fig. 6. The dominance of the recoil limit is evident for any realistic value of the laser power at a moderately large waist of 20 μm and for 10^5 fermions. The heating limit does not depend on the waist of the laser beam since both the scattering rate and the Fermi energy scale as an inverse square power of the waist; however, larger number of fermions will increase E_F with different scalings for the two bounds E_R/E_F and $(T/T_F)_{\rm min}$ (proportional to $N_F^{-1/3}$ and to $N_F^{-1/6}$, respectively), making the limitation due to heating progressively more relevant.

The numerical examples reported here are not fully optimized as they are chosen with an eye towards trapping performances already achieved in various laboratories. Given the high degree of nonlinearity in the protocol and the dependence on the relevant parameters, improvements by at least one order of magnitude with respect to the estimated degeneracy parameter, could be realistically achievable in specific configurations. The cooling time scale—as visible in Fig. 5—seems short, at least for the specific case of the ^{6}Li transition used as an example. However, more elaborated cooling cycles based upon repeatedly ramping up and down the laser power may extend the lifetime of the ultracold

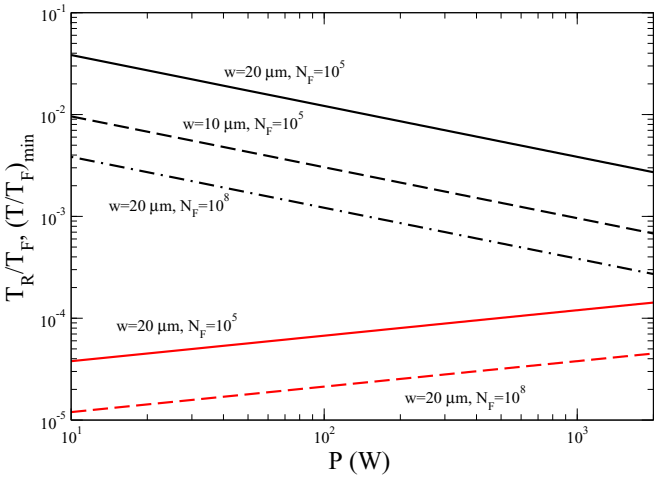

FIG. 6. Limits to the degeneracy factor T/T_F arising from the recoil limit (three top black curves) and the heating and cooling rates estimated in the text through Eq. (9) (two bottom red curves), versus the laser power and for various values of the beam waist and number of fermions. The parameters are the same as for the $2s_{1/2} - 2p_{3/2}$ cyclic transition discussed in Fig. 4.

sample well beyond the millisecond scale. Considering the large trapping frequencies achieved in high-power ODTs, and the fact that the inverse of the chemical potential usually determines the time scale for building up strongly correlated phases, we do not expect the cooling time scale to be an issue in the study of several phase transitions predicted so far in the ultracold regime. Even without fully optimizing the many parameters available, a final degeneracy factor T/T_F below the 10^{-2} range seems within reach, as can be seen, in particular, looking at the limits in Fig. 6.

V. CONCLUSIONS

In conclusion, we have discussed an experimental setup in which a peculiar feature of degenerate Fermi gases, the expected narrowing of the spontaneous emission linewidth, may be exploited as a cooling mechanism. The same advantages of all-optical cooling of atomic gases discussed elsewhere do apply here, without the loss of atoms as in dual evaporative cooling, the complication of simultaneous trapping of a Bose gas with large heat capacity as in sympathetic cooling, and with the possibility to fully exploit Feshbach resonances. The concurrent suppression of light scattering expected for a degenerate Fermi gas also has two added benefits. First, the reduced radiation pressure experienced by the atoms allows for higher atomic densities, and atomic heating by light scattering is suppressed in the strong confinement provided by the ODT, as experimentally demonstrated in an optical lattice [25]. Second, continuous and precision monitoring of the cloud temperature through off-resonant beams over the duration of the experiment [21] helps to mitigate another critical issue for degenerate Fermi gases, namely, the lack of sensitive precision thermometry in the degenerate regime, a crucial point for the study of classical phase transitions [2].

The use of tight trapping conditions makes this cooling scheme less palatable for the application to optical lattices in which a degree of spatial homogeneity is often a prerequisite for creating and observing unconventional phases. However, the combination of this cooling mechanism with adiabatic expansions, such as the ones designed through frictionless cooling [26,27], should mitigate this drawback. Moreover, a direct implementation of Pauli blocking schemes to further cooling in optical lattices seems feasible [28].

A full expansion of the proposal should also include a treatment of the dynamics of the atoms in a combined MOT-ODT configuration, as this gives rise to confinements rather different in various spatial regions, with a small, inner region experiencing stiff confinement and a large, outer region loosely confined, and not contributing to the cooling effect exploited in this scheme. The proposal could take advantage of efforts to produce a large volume ODT [29,30], also complementing existing demonstrations of efficient all-optical cooling of atomic gases, either alkaline-earth metals [31–34], or fermionic isotopes of lithium and potassium [35–37] via intrinsically narrow transitions. The experiment described in [24] seems the closest, both in the setup and parameters space, to a successful implementation of the technique proposed in this paper. From a broader, fundamental physics standpoint, implementing this cooling technique should also yield a beautiful macroscopic demonstration of the Pauli principle, complementing recently reported evidence of microscopic character [38].

ACKNOWLEDGMENTS

I am grateful to Lorenza Viola and Kevin C. Wright for a critical reading of the manuscript.

[1] I. Bloch, Ultracold quantum gases in optical lattices, Nat. Phys. **1**, 23 (2005).
[2] D. C. McKay and B. DeMarco, Cooling in strongly correlated optical lattices: Prospects and challenges, Rep. Prog. Phys. **74**, 054401 (2011).
[3] M. Lewenstein, A. Sampera, and V. Ahufinger, *Ultracold Atoms in Optical Lattices* (Oxford University Press, New York, 2012).
[4] Y. Shin, C. H. Schunck, A. Schirotzek, and W. Ketterle, Phase diagram of a two-component Fermi gas with resonant interactions, Nature (London) **451**, 689 (2008).
[5] G. B. Partridge, W. Li, R. I. Kamar, Y.-A. Liao, and R. G. Hulet, Pairing and phase separation in a polarized Fermi gas, Science **311**, 503 (2006).
[6] E. Timmermans, Degenerate Fermion Gas Heating by Hole Creation, Phys. Rev. Lett. **87**, 240403 (2001).
[7] M. Crescimanno, C. G. Kaoy, and R. Peterson, Limits to evaporative cooling of a two-component Fermi gas, Phys. Rev. A **61**, 053602 (2000).
[8] M. J. Holland, B. DeMarco, and D. S. Jin, Evaporative cooling of a two-component degenerate Fermi gas, Phys. Rev. A **61**, 053610 (2000).

[9] B. DeMarco and D. S. Jin, Onset of Fermi degeneracy in a trapped atomic gas, Science **285**, 1703 (1999).

[10] A. G. Truscott, K. E. Strecker, W. I. McAlexander, G. B. Partridge, and R. G. Hulet, Observation of Fermi pressure in a gas of trapped atoms, Science **291**, 2570 (2001).

[11] R. Onofrio and C. Presilla, Reaching Fermi Degeneracy in Two-Species Optical Dipole Traps, Phys. Rev. Lett. **89**, 100401 (2002).

[12] C. Presilla and R. Onofrio, Cooling Dynamics of Ultracold Two-Species Fermi-Bose Mixtures, Phys. Rev. Lett. **90**, 030404 (2003).

[13] J. Catani, G. Barontini, G. Lamporesi, F. Rabatti, G. Thalhammer, F. Minardi, S. Stringari, and M. Inguscio, Entropy Exchange in a Mixture of Ultracold Atoms, Phys. Rev. Lett. **103**, 140401 (2009).

[14] F. Baumer, F. Münchow, A. Görlitz, S. E. Maxwell, P. S. Julienne, and E. Tiesinga, Spatial separation in a thermal mixture of ultracold ^{174}Yb and ^{87}Rb atoms, Phys. Rev. A **83**, 040702(R) (2011).

[15] V. D. Vaidya, J. Tiamsuphat, S. L. Rolston, and J. V. Porto, Degenerate Bose-Fermi mixtures of rubidium and ytterbium, Phys. Rev. A **92**, 043604 (2015).

[16] K. Helmerson, M. Xiao, and D. Pritchard, *Radiative decay of densely confined atoms*, International Quantum Electronics Conference 1990, book of abstracts, OSA Technical Digest (Optical Society of America, Washington, D.C., 1990), paper QTHH4.

[17] A. Imamoglu and L. You, Many-body quantum Monte Carlo wave-function approach to the dissipative atom-field interaction, Phys. Rev. A **50**, 2642 (1994).

[18] J. Javanainen and J. Ruostekoski, Off-resonance light scattering from low-temperature Bose and Fermi gases, Phys. Rev. A **52**, 3033 (1995).

[19] Th. Busch, J. R. Anglin, J. I. Cirac, and P. Zoller, Inhibition of spontaneous emission in Fermi gases, Europhys. Lett. **44**, 1 (1998).

[20] A. Görlitz, A. P. Chikkatur, and W. Ketterle, Enhancement and suppression of spontaneous emission and light scattering by quantum degeneracy, Phys. Rev. A **63**, 041601(R) (2001).

[21] B. Shuve and J. H. Thywissen, Enhanced Pauli blocking of light scattering in a trapped Fermi gas, J. Phys. B **43**, 015301 (2010).

[22] C. D. Herold, V. D. Vaidya, X. Li, S. L. Rolston, J. V. Porto, and M. S. Safronova, Precision Measurement of Transition Matrix Elements via Light Shift Cancellation, Phys. Rev. Lett. **109**, 243003 (2012).

[23] M. S. Safronova, U. I. Safronova, and C. W. Clark, Magic wavelengths for optical cooling and trapping of lithium, Phys. Rev. A **86**, 042505 (2012).

[24] A. Burchianti, G. Valtolina, J. A. Seman, E. Pace, M. De Pas, M. Inguscio, M. Zaccanti, and G. Roati, Efficient all-optical production of large ^{6}Li quantum gases using D_1 gray-molasses cooling, Phys. Rev. A **90**, 043408 (2014).

[25] S. Wolf, S. J. Oliver, and D. S. Weiss, Suppression of Recoil Heating by an Optical Lattice, Phys. Rev. Lett. **85**, 4249 (2000).

[26] X. Chen, A. Ruschhaupt, S. Schmidt, A. del Campo, D. Guéry-Odelin, and J. G. Muga, Fast Optimal Frictionless Cooling in Harmonic Traps: Shortcuts to Adiabaticity, Phys. Rev. Lett. **104**, 063002 (2010).

[27] E. Torrontegui, S. Ibáñez, S. Martínez-Garaot, M. Modugno, A. del Campo, D. Guéry-Odelin, A. Ruschhaupt, X. Chen, and J. G. Muga, Shortcuts to adiabaticity, Adv. At., Mol., Opt. Phys. **62**, 117 (2013).

[28] R. M. Sandner, M. Müller, A. J. Daley, and P. Zoller, Spatial Pauli blocking of spontaneous emission in optical lattices, Phys. Rev. A **84**, 043825 (2011).

[29] A. Mosk, S. Jochim, H. Moritz, Th. Elsässer, and M. Weidenmüller, Resonator-enhanced optical dipole trap for fermionic lithium atoms, Opt. Lett. **26**, 1837 (2001).

[30] S. Stellmer, B. Pasquiou, R. Grimm, and F. Schreck, Laser Cooling to Quantum Degeneracy, Phys. Rev. Lett. **110**, 263003 (2013).

[31] H. Katori, T. Ido, Y. Isoya, and M. Kutawa-Gonokami, Magneto-Optical Trapping and Cooling of Strontium Atoms down to the Photon Recoil Temperature, Phys. Rev. Lett. **82**, 1116 (1999).

[32] T. Binnewies, G. Wilpers, U. Sterr, F. Riehle, J. Helmcke, T. E. Mehlstäubler, E. M. Rasel, and W. Ertmer, Doppler Cooling and Trapping on Forbidden Transitions, Phys. Rev. Lett. **87**, 123002 (2001).

[33] E. A. Curtis, C. W. Oates, and L. Hollberg, Quenched narrow-line laser cooling of ^{40}Ca to near the photon recoil limit, Phys. Rev. A **64**, 031403 (2001).

[34] T. H. Loftus, T. Ido, A. D. Ludlow, M. M. M. Boyd, and J. Ye, Narrow Line Cooling: Finite Photon Recoil Dynamics, Phys. Rev. Lett. **93**, 073003 (2004).

[35] P. M. Duarte, R. A. Hart, J. M. Hitchcock, T. A. Corcovilos, T.-L. Yang, A. Reed, and R. G. Hulet, All-optical production of a lithium quantum gas using narrow-line laser cooling, Phys. Rev. A **84**, 061406(R) (2011).

[36] D. C. McKay, D. Jervis, D. J. Fine, J. W. Simpson-Porco, G. J. A. Edge, and J. H. Thywissen, Low-temperature high-density magneto-optical trapping of potassium using the open $4S \rightarrow 5P$ transition at 405 nm, Phys. Rev. A **84**, 063420 (2011).

[37] J. Sebastian, Ch. Gross, Ke Li, H. C. J. Gan, Wenhui Li, and K. Dieckmann, Two-stage magneto-optical trapping and narrow-line cooling of ^{6}Li atoms to high phase-space density, Phys. Rev. A **90**, 033417 (2014).

[38] A. Omran, M. Boll, T. A. Hilker, K. Kleinlein, G. Salomon, I. Bloch, and C. Gross, Microscopic Observation of Pauli Blocking in Degenerate Fermionic Lattice Gases, Phys. Rev. Lett. **115**, 263001 (2015).